

# Entanglement entropy and multifractality at localization transitions

Xun Jia,<sup>1</sup> Arvind R. Subramaniam,<sup>2</sup> Ilya A. Gruzberg,<sup>2</sup> and Sudip Chakravarty<sup>1</sup>

<sup>1</sup>*Department of Physics and Astronomy, University of California Los Angeles, Los Angeles, CA 90095-1547*

<sup>2</sup>*James Franck Institute and Department of Physics, University of Chicago, Chicago, IL 60637*

(Dated: October 08, 2007)

The von Neumann entanglement entropy is a useful measure to characterize a quantum phase transition. We investigate the non-analyticity of this entropy at disorder-dominated quantum phase transitions in non-interacting electronic systems. At these critical points, the von Neumann entropy is determined by the single particle wave function intensity which exhibits complex scale invariant fluctuations. We find that the concept of multifractality is naturally suited for studying von Neumann entropy of the critical wave functions. Our numerical simulations of the three dimensional Anderson localization transition and the integer quantum Hall plateau transition show that the entanglement at these transitions is well described using multifractal analysis.

Entanglement is a unique feature of a quantum system and entanglement entropy, defined through the von Neumann entropy (vNE) measure, is one of the most widely used quantitative measures of entanglement [1, 2, 3, 4]. Consider a composite system that can be partitioned into two subsystems  $A$  and  $B$ . The vNE of either of the subsystems is  $s_A = -\text{Tr}_A \rho_A \ln \rho_A = s_B = -\text{Tr}_B \rho_B \ln \rho_B$ . Here, the reduced density matrix  $\rho_A$  is obtained by tracing over the degrees of freedom in  $B$ :  $\rho_A = \text{Tr}_B |\psi_{AB}\rangle\langle\psi_{AB}|$  and similarly for  $\rho_B$ . In general, for a pure state  $|\psi_{AB}\rangle$  of a composite system, the reduced density matrix is a mixture, and the corresponding entropy is a good measure of entanglement.

The scaling behavior of entanglement entropy is a particularly useful characterization near a quantum phase transition [2]. The entanglement entropy can show non-analyticity at the phase transition even when the ground state energy (the quantum analog of the classical free energy) is analytic. While these ideas have been studied in a number of translation-invariant models [2, 3, 5], there have been far fewer investigations of random quantum critical points (for notable exceptions, see [6]).

In particular, non-interacting electrons moving in a disordered potential, can undergo continuous quantum phase transitions between an extended, metallic and a localized, insulating state as the Fermi energy is varied across a critical energy,  $E_C$ . Well known examples are the Anderson transition in three dimensions (3D) and the integer quantum Hall (IQH) plateau transition in two dimensions where the ground state energy does not exhibit any non-analyticity. In contrast, vNE will be shown to exhibit non-analyticity at these transitions and a scaling behavior. At the outset it should be emphasized that because of the single particle and disorder-dominated nature of these quantum phase transitions, entanglement as characterized by vNE and its critical scaling behavior, are fundamentally different from those calculated for interacting systems. This statement will be made more precise later.

In a non-interacting electronic system close to a disordered critical point, the wave function intensity at en-

ergy  $E$ ,  $|\psi_E(r)|^2$  fluctuates strongly at each spatial point  $r$  and consequently has a broad (non-Gaussian) distribution even in the thermodynamic limit [7]. This non self-averaging nature of the wave function intensity is characterized through the scaling of its moments. In particular, moments of normalized wave function intensity,  $P_q$  (called the generalized inverse participation ratios) obey the finite-size scaling ansatz,

$$P_q(E) \equiv \sum_r \overline{|\psi_E(r)|^{2q}} \sim L^{-\tau_q} \mathcal{F}_q[(E - E_C)L^{1/\nu}]. \quad (1)$$

Here  $L$  is the system size,  $\nu$  is the exponent characterizing the divergence of correlation length,  $\xi_E \sim |E - E_C|^{-\nu}$ .  $\tau_q$  is called the multifractal spectrum and the overbar denotes averaging over different disorder realizations.  $\mathcal{F}_q(x)$  is a scaling function with  $\mathcal{F}_q(x \rightarrow 0) = 1$  close to the critical point  $E = E_C$ . When  $E$  is tuned away from  $E_C$ , the system either tends towards an ideal metallic state with  $P_q(E) \sim L^{-D(q-1)}$  ( $D$  being the number of spatial dimensions) or becomes localized with  $P_q(E)$  independent of  $L$ .

Below, we first show that the disorder-averaged vNE can be expressed as a derivative of  $P_q$  and thus its scaling behavior follows from multifractal analysis. After that, we apply our formalism to understand the numerical results on vNE at the 3D Anderson localization and IQH plateau transitions. vNE in the Anderson localization problem was studied previously [4, 8] but the connection with multifractality and the unique features of vNE at these quantum phase transitions have not been clearly elucidated.

Even though the disorder induced localization problem can be studied in a single particle quantum mechanics language, there is no obvious way to define entanglement entropy in this picture. However (see Ref. [9]), entanglement can be defined using the site occupation number basis in the second-quantized Fock space. Let us divide the lattice of linear size  $L$  into two regions  $A$  and  $B$ . A single particle eigenstate of a lattice Hamiltonian at energy  $E$  is represented in the site occupation number basis

as

$$|\psi_E\rangle = \sum_{r \in A \cup B} \psi_E(r) |1\rangle_r \bigotimes_{r' \neq r} |0\rangle_{r'} \quad (2)$$

Here  $\psi_E(r)$  is the normalized single particle wave function at site  $r$  and  $|n\rangle_r$  denotes a state having  $n$  particles at site  $r$ . We decompose the above sum over lattice sites  $r$  into the mutually orthogonal terms,

$$|\psi_E\rangle = |1\rangle_A \otimes |0\rangle_B + |0\rangle_A \otimes |1\rangle_B \quad (3)$$

where

$$|1\rangle_A = \sum_{r \in A} \psi_E(r) |1\rangle_r \bigotimes_{r' \neq r} |0\rangle_{r'}, \quad |0\rangle_A = \bigotimes_{r \in A} |0\rangle_r \quad (4)$$

with analogous expressions for the  $|1\rangle_B$  and  $|0\rangle_B$  states. Notice that these states have the normalization

$$\langle 0|0\rangle_A = \langle 0|0\rangle_B = 1, \quad \langle 1|1\rangle_A = p_A, \quad \langle 1|1\rangle_B = p_B, \quad (5)$$

where

$$p_A = \sum_{r \in A} |\psi_E(r)|^2, \quad (6)$$

and similarly for  $p_B$  with  $p_A + p_B = 1$ .

To obtain the reduced density matrix  $\rho_A$ , we trace out the Hilbert space over  $B$  in the density matrix  $\rho = |\psi_E\rangle\langle\psi_E|$ . This gives,

$$\rho_A = |1\rangle_A\langle 1| + p_B |0\rangle_A\langle 0|. \quad (7)$$

The corresponding vNE is given by

$$s_A = -p_A \ln p_A - p_B \ln p_B. \quad (8)$$

In the above equation, we see that manifestly  $s_A = s_B$ . More importantly,  $s_A$  is bounded between 0 and  $\ln 2$  for any eigenstate. This is in sharp contrast to the entanglement entropy in interacting quantum systems where it can be arbitrarily large near the critical point. The reason for this is also clear: Even though we used a second-quantized language, we are dealing with a single particle state rather than a many body correlated state. Consequently the entanglement entropy does not grow arbitrarily large as a function of the size of  $A$ .

We also observe that at criticality, if the whole system size becomes very large in comparison with the subsystem  $A$ , we can restrict the subsystem to be a single lattice site and study the scaling dependence w.r.t the overall system size  $L$ . Then using the ansatz of scale invariance, we can always find the scaling of the entanglement as a function of the subsystem size  $l$  since near criticality, only the dimensionless ratio  $L/l$  can enter any physical quantity. To extract scaling, we find the bipartite entanglement of a single site  $r$  with the rest of the system and sum this

over all lattice sites in the system. Using Eq. (8) we write this as

$$S(E) = - \sum_{r \in L^d} \left[ |\psi_E(r)|^2 \ln |\psi_E(r)|^2 + (1 - |\psi_E(r)|^2) \ln (1 - |\psi_E(r)|^2) \right]. \quad (9)$$

To leading order, the second term inside the square bracket in Eq. (9) can be dropped, since  $|\psi_E(r)|^2 \ll 1$  at all points  $r$  when the states are close to the critical energy. We can readily relate the disorder average (denoted by overbar) of this entropy to the multifractal scaling in Eq. (1) and get the  $L$  scaling as,

$$\bar{S}(E) \approx - \left. \frac{dP_q}{dq} \right|_{q=1} \approx \left. \frac{d\tau_q}{dq} \right|_{q=1} \ln L - \left. \frac{\partial \mathcal{F}_q}{\partial q} \right|_{q=1}. \quad (10)$$

We do not know the general form of the scaling function  $\mathcal{F}_q$  but we can get the approximate  $L$  dependence of the entropy in various limiting cases. For the exactly critical case when  $\mathcal{F}_q \equiv 1$  for all values of  $q$ , we get

$$\bar{S}(E) \sim \alpha_1 \ln L, \quad (11)$$

where the constant  $\alpha_1 = d\tau_q/dq|_{q=1}$  is unique for each universality class. From the discussion following Eq. (1), the leading scaling behavior of  $\bar{S}(E)$  in the ideal metallic and localized states is given by  $D \ln L$  and  $\alpha_1 \ln \xi_E$  respectively. From the limiting cases, we see that in general,  $\bar{S}(E)$  has the approximate form

$$\bar{S}(E) \sim \mathcal{K}[(E - E_C)L^{1/\nu}] \ln L, \quad (12)$$

where the coefficient function  $\mathcal{K}(x)$  decreases from  $D$  in the metallic state to  $\alpha_1$  at criticality and then drops to zero for the localized state. We will see that this scaling form is verified in our numerical simulations.

The scaling form for the entanglement entropy averaged over all eigenstates of the single particle Hamiltonian is also of interest since this scaling can change as a function of disorder strength. To be specific, let us consider the 3D Anderson model on a cubic lattice. The Hamiltonian is,

$$H = \sum_i V_i c_i^\dagger c_i - t \sum_{\langle i,j \rangle} (c_i^\dagger c_j + h.c) \quad (13)$$

where  $c_i^\dagger(c_i)$  is the fermionic creation (annihilation) operator at the site  $i$  of the lattice, and the second sum is over all nearest neighbors. We set  $t = 1$  and the  $V_i$  are random variables uniformly distributed in the range  $[-W/2, W/2]$ . It is known [10] that as  $W$  is decreased from a very high value, extended states appear at the band center below the critical disorder strength  $W_c = 16.3$ , and a recent work [11] reported the localization length exponent  $\nu = 1.57 \pm 0.03$ .

The analysis leading to Eq. (12) also holds when we study wave functions at a single energy, say  $E = 0$  and

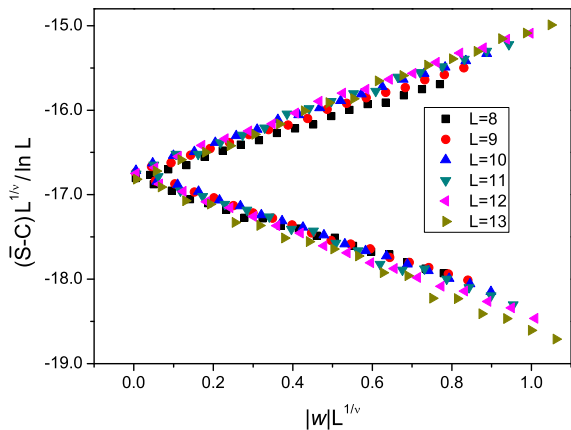


FIG. 1: Scaling curve in the 3D Anderson model. With the choice of  $\nu = 1.57$  and  $C = 12.96$ , all data collapse to a universal functions  $f_{\pm}(x)$ . The two branches correspond to  $w < 0$  and  $w > 0$ .

increase the disorder strength in the Anderson model across the critical value  $W_c$ . In this case, the states at  $E = 0$  evolve continuously from fully metallic to critical and then finally localized, resulting in the approximate form for the entanglement entropy as

$$\overline{S}(E = 0, w, L) \sim \mathcal{C}(wL^{1/\nu}) \ln L, \quad (14)$$

where  $w = (W - W_c)/W_c$  is the normalized relative disorder strength and  $\mathcal{C}(x)$  is a scaling function. In particular, as mentioned before,  $\mathcal{C}(x) \rightarrow D$  as  $w \rightarrow -1$ ,  $\mathcal{C}(x) \rightarrow 0$  as  $w \rightarrow \infty$ , and  $\mathcal{C}(x) = \alpha_1$  when  $w = 0$ .

Next, we look at the energy-averaged entropy. We average Eq. (10) over the entire band of energy eigenvalues and construct the vNE,

$$\overline{S}(w, L) = \frac{1}{L^3} \sum_E \overline{S}(E, w, L), \quad (15)$$

where  $L^3$  is also the total number of states in the band. Then using Eq. (12) and Eq. (14), one can show that close to  $w = 0$ ,

$$\overline{S}(w, L) \sim C + L^{-1/\nu} f_{\pm}(wL^{1/\nu}) \ln L \quad (16)$$

where  $C$  is an  $L$  independent constant, and  $f_{\pm}(x)$  are two universal functions corresponding to the two regimes  $w > 0$  and  $w < 0$ .

We numerically diagonalize the Hamiltonian (13) in a finite  $L \times L \times L$  system with periodic boundary conditions. The maximum system size is  $L = 13$  and the results are averaged over 20 disorder realizations. The scaling form of  $\overline{S}(w, L)$  is given by (16). Figure 1 shows the results of the data collapse with a choice of  $\nu = 1.57$ , and the nonuniversal constant  $C = 12.96$  is determined by a powerful algorithm described in Ref. [12]. The successful data collapse reflects the non-analyticity of the von Neumann entropy and accuracy of the multifractal analysis.

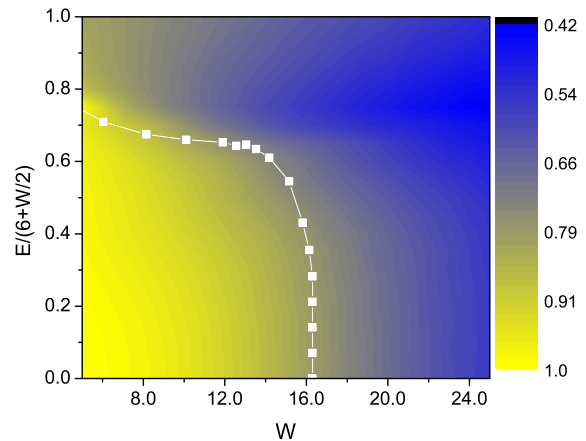


FIG. 2:  $\overline{S}(E, W, L)$  as a function of  $E$  and  $W$  computed in a system with  $L = 10$ . The square shows the mobility edge reported in Ref. [14]. Because of the finiteness of the system, the transition from the localized to the delocalized region is smooth.

We also use the transfer matrix method [13] to study the energy dependence of  $\overline{S}(E, w, L)$  by considering a quasi-1D system with a size of  $(mL) \times L \times L$ ,  $m \gg 1$ . We use  $L$  up to 18, and  $m = 2000 \gg 1$  is found to be sufficient. To compute vNE, we divide the quasi-1D system into  $m$  cubes labeled by  $I = 1, 2, \dots, m$ , each containing  $L^3$  sites. We normalize the wave function within each cube and compute the vNE,  $\overline{S}^I(E, W, L)$ , in the  $I^{\text{th}}$  cube, and finally  $\overline{S}(E, W, L)$  is obtained by averaging over all cubes.

A typical  $\overline{S}(E, W, L)$  with  $L = 10$  is shown in Fig. 2. The value of  $\overline{S}(E, W, L)$  is normalized by  $\ln(L^3)$  such that  $\overline{S} \rightarrow 1$  in a fully extended state. The energy  $E$  is normalized by  $(W/2 + 6)$ , which is the energy range of non-zero density of states [15]. The mobility edge computed in Ref. [14] is also plotted in Fig. 2. The validity of the scaling form in Eq. (14) is seen in Fig. 3. In particular, the function  $\mathcal{C}(x)$  shows the expected behavior.

Consider now the second example, the integer quantum Hall system in a magnetic field  $B$ . The Hamiltonian can be expressed [16] in terms of the matrix elements of the states  $|n, k\rangle$ , where  $n$  is the Landau level index, and  $k$  is the wave vector in the  $y$  direction. Focussing on the lowest Landau level  $n = 0$ , with the impurity distribution  $\overline{V}(\mathbf{r})\overline{V}(\mathbf{r}') = V_0^2 \delta(\mathbf{r} - \mathbf{r}')$ , the matrix element  $\langle 0, k | V | 0, k' \rangle$  can be generated as in Ref. [16].

Now consider a 2D square with a linear dimension  $L = \sqrt{2\pi} M l_B$ , where  $l_B = (\hbar/eB)^{1/2}$  is the magnetic length and  $M$  is an integer, with periodic boundary conditions imposed in both directions. We discretize the system with a mesh of size  $\sqrt{\pi} l_B / \sqrt{2} M$ . The Hamiltonian matrix is diagonalized and a set of eigenstates  $\{|\psi_a\rangle = \sum_k \alpha_{k,a} |0, k\rangle\}_{a=1}^{M^2}$  is obtained with corresponding eigenvalues  $\{E_a\}_{a=1}^{M^2}$ . The energies are measured relative to the center of the lowest Landau band [17] in units of  $\Gamma = 2V_0 / \sqrt{2\pi} l_B$ . Finally, for each eigenstate the wave

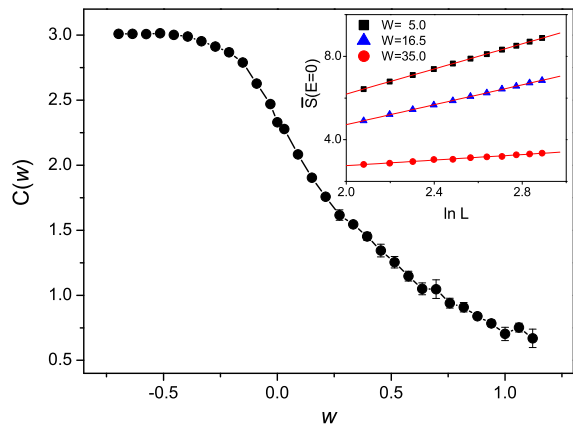


FIG. 3: The quantity  $\mathcal{C}$  in Eq. (14). The range of the system sizes is too small to observe the weak  $L$ -dependence. Inset:  $\overline{S}(E=0, W, L)$  as a function of  $\ln L$  for 3 different  $W$ .

function in real space can be constructed as:

$$\psi_a(x, y) = \langle x, y | \psi_a \rangle = \sum_k \alpha_{k,a} \psi_{0,k}(x, y) \quad (17)$$

where  $\psi_{0,k}(x, y)$  is the lowest Landau level wave function with a momentum quantum number  $k$ .

The dimension of the Hamiltonian matrix increases as  $N_k \sim M^2$ , making it difficult to diagonalize fully. Instead we compute only those states  $|\psi_a\rangle$  whose energies lie in a small window  $\Delta$  around a preset value  $E$ , i.e.  $E_a \in [E - \Delta/2, E + \Delta/2]$ . We ensure that  $\Delta$  is sufficiently small (0.01) while at the same time, there are enough states in the interval  $\Delta$  (at least 100 eigenstates).

We now uniformly break up the  $L \times L$  square into nonoverlapping squares  $\mathcal{A}_i$  of size  $l \times l$ , where  $l = l_B \sqrt{\pi/2}$  independent of the system size  $L$ . For each of the states, we compute the coarse grained quantity  $\int_{(x,y) \in \mathcal{A}_i} |\psi_a(x, y)|^2 dx dy$ . The computation of the vNE for a given eigenstate follows the same procedure described for the Anderson localization. Finally, by averaging over states in the interval  $\Delta$ , the vNE  $\overline{S}(E, L)$  is obtained at the preset energy  $E$ . The scaling form of  $\overline{S}(E, L)$  is given by Eq. (12) with  $E_C = 0$  and is  $\overline{S}(E, L) = \mathcal{K}(|E|L^{1/\nu}) \ln L$ . Good agreement with the numerical simulations is seen in Fig. 4.

In conclusion, we have clearly established the formalism for computing the entanglement entropy near quantum critical points in non-interacting disordered electronic systems. We have also identified its relation with the well-studied notion of multifractality and illustrated our concepts through numerical simulations of two important models, the 3D Anderson transition and the IQH plateau transition. This work represents a starting point to study entanglement in electronic systems with both disorder and interactions.

This work was supported by NSF grant DMR-0705092 (SC and XJ), NSF MRSEC Program under DMR-0213745, the NSF Career grant DMR-0448820 and the

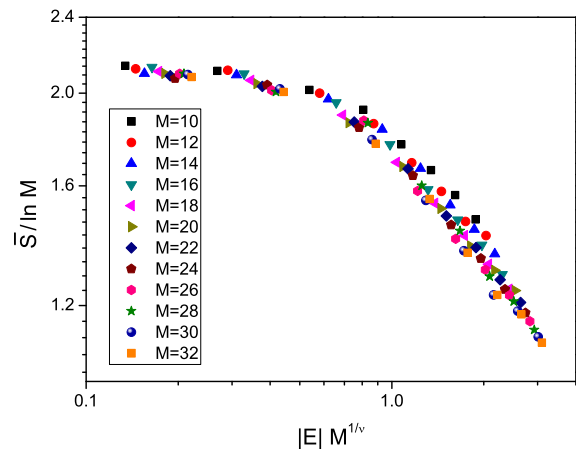


FIG. 4: Scaling of the von Neumann entropy  $\overline{S}(E, L)$  for the IQHE.  $M$  instead of  $L$  is used in the data collapse with the accepted value of  $\nu = 2.33$ .

Research Corporation (IAG and ARS). ARS and IAG acknowledge hospitality at the Institute for Pure and Applied Mathematics, UCLA where this work was started. SC would also like to thank the Aspen Center for Physics.

- [1] T. Osborne and M. Nielsen, Phys. Rev. A **66**, 32110 (2002); A. Kitaev and J. Preskill, Phys. Rev. Lett. **96**, 110404 (2006); M. Levin and X.-G. Wen, Phys. Rev. Lett. **96**, 110405 (2006); M. Haque, O. Zozulya, and K. Schoutens, Phys. Rev. Lett. **98**, 60401 (2007); L. Amico *et al.*, arXiv:0706.3737.
- [2] G. Vidal *et al.*, Phys. Rev. Lett. **90**, 227902 (2003).
- [3] P. Calabrese and J. Cardy, J. Stat. Mech. **6**, 2 (2004).
- [4] A. Kopp, X. Jia, and S. Chakravarty, Ann. Phys. **322**, 1466 (2007).
- [5] L. A. Wu, M. S. Sarandy, and D. A. Lidar, Phys. Rev. Lett. **93**, 250404 (2004); E. Fradkin and J. E. Moore, Phys. Rev. Lett. **97**, 50404 (2006).
- [6] G. Refael and J. E. Moore, Phys. Rev. Lett. **93**, 260602 (2004); R. Santachiara, J. Stat. Mech. **06**, L002 (2006); N. E. Bonesteel and K. Yang, Phys. Rev. Lett. **99**, 140405 (2007).
- [7] C. Castellani and L. Peliti, J. Phys. A **19**, L429 (1986); F. Evers and A. D. Mirlin, arXiv:0708.4378.
- [8] I. Varga and J. A. Mendez-Bermudez, arXiv:0708.3682.
- [9] P. Zanardi, Phys. Rev. A **65**, 42101 (2002).
- [10] A. MacKinnon and B. Kramer, Phys. Rev. Lett. **47**, 1546 (1981).
- [11] K. Slevin, P. Markos, and T. Ohtsuki, Phys. Rev. Lett. **86**, 3594 (2001).
- [12] P. Goswami, X. Jia, and S. Chakravarty, Phys. Rev. B (to be published); arXiv:0706.3737 (refer Appendix C).
- [13] B. Kramer and M. Schreiber, in *Computational Physics*, edited by K. H. Hoffmann and M. Schreiber (Springer, Berlin, 1996), p. 166.
- [14] B. Bulka, M. Schreiber, and B. Kramer, Z. Phys. B **66**, 21 (1987).
- [15] F. Wegner, Z. Phys. B **44**, 9 (1981).
- [16] B. Huckestein, Rev. Mod. Phys. **67**, 357 (1995).
- [17] T. Ando and Y. Uemura, J. Phys. Soc. Jpn. **36**, 959 (1974).